



## Specific UV–vis absorbance changes of humic acid in the presence of clay particles during photocatalytic oxidation

Sibel Sen Kavurmaci\*, Miray Bekbolet

*Institute of Environmental Sciences, Bogazici University, 34342 Bebek, Istanbul, Turkey*  
Tel. +90 212 359 7145; Fax: +90 212 257 5033; email: sibel.sen@boun.edu.tr

Received 18 January 2013; Accepted 21 March 2013

### ABSTRACT

Photocatalytic oxidation of humic acid (HA) in the presence of clay particles (montmorillonite [Mt] or kaolinite [Kt]) followed using specific UV–vis parameters ( $SUVA_{365}$ ,  $SUVA_{280}$ ,  $SUVA_{254}$ , and SCoA) calculated by respective absorbance measurements through conversion to mass of carbon. Non-selective oxidative degradation of HA could be displayed by the observed changes in the UV–vis spectral features in accordance with the successful elimination of the dissolved organic carbon. It was previously reported that fractional UV–vis parameters ( $E_{254}/E_{365}$ ,  $E_{254}/E_{436}$ ,  $E_{280}/E_{365}$ ,  $E_{280}/E_{436}$ , and  $E_{365}/E_{436}$ ) could signify the removal of color forming groups in relation to the removal of UV absorbing centers revealing information on the different oxidation pathways through photocatalysis. Regarding the results attained in this study, with respect to the changes attained in the specific UV–vis parameters, it could be indicated that the photocatalytic oxidation mechanism was significantly different for HA in the presence of either Mt or Kt. No noteworthy variation could be detected for fractional UV–vis parameters under photocatalytic conditions for sole HA as well as for HA in the presence of either Mt or Kt. However, a significant correlative interaction was observed between the specific UV–vis parameters ( $SUVA_{254}$  and SCoA) and the fractional UV–vis parameter ( $E_{254}/E_{436}$ ) ( $r^2 > 0.80$ ). Therefore, it could be concluded that  $E_{365}/E_{436}$  parameter could be successfully used as a discriminative indicator parameter of the specific UV–vis parameters for the photocatalytic degradation of HA in the presence of either Mt or Kt.

*Keywords:* Photocatalytic oxidation; Humic acid; Specific and fractional UV–vis parameters; Montmorillonite and kaolinite

### 1. Introduction

Photocatalytic oxidation of humic acid (HA) displays a recent interest due to the complex properties of organic matrix representing both natural organic matter (NOM), as well as, wastewater-originated composite organic substrates. NOM components are

classified according to their pH depending solubilities, mainly as HA, that are soluble under neutral and alkaline conditions [1]. The ill-defined nature of HA holds significance due to its reactivity towards oxidative treatment through which conformational and structural changes could be expected in accordance with the successive removal of dissolved organic carbon (DOC) [1]. Because of the presence of various chromophoric groups the spectral properties of humic

\*Corresponding author.

substances have been studied extensively. NOM more specifically HAs express UV–vis characteristics as decreasing absorption with increasing wavelength in an approximately exponential fashion [2,3]. The presence of unsaturated compounds with delocalized lone pair of electrons usually imparts a distinct yellowish color to the water, and ultraviolet-visible (UV–vis) light-spectroscopy could therefore be used to estimate the absorbing compounds properties as well as removals, by treatment [4,5].

UV–vis spectroscopic profiles of model HAs expressed a featureless trend with respect to increasing wavelength, irrespective of the source and origin of the substrates under non-oxidative, as well as oxidative conditions [4–6]. Besides the oxidation of various sole HAs, the possible role of the natural water constituents had also been studied in detail and compiled in a recent review article by Uyguner Demirel and Bekbolet [7]. With reference to the natural water colloidal systems, the effect of clay particles on the photocatalytic oxidation of HAs deserves to be investigated. Kinetic modeling and oxidation efficiency of photocatalytic oxidation of HA in the presence of either Mt or Kt have been reported elsewhere [8,9]. In this study, a complementary approach is presented indicating the use of the specific UV absorbance parameters to provide further insight to the photocatalytic degradation of HA [10,11]. Moreover, fractional UV–vis absorbance parameters (i.e.  $E_{254}/E_{365}$ ,  $E_{254}/E_{436}$ ,  $E_{280}/E_{365}$ ,  $E_{280}/E_{436}$ , and  $E_{365}/E_{436}$ ) were also investigated. The main purpose was to elucidate the role of UV–vis spectral features in relation to DOC removals for the assessment of the non-selective oxidation of HA in the presence of either Mt or Kt.

## 2. Materials and methods

### 2.1. Materials

HA (supplied from Aldrich) solution ( $50 \text{ mgL}^{-1}$ ) was prepared by dilution of the stock solution ( $1,000 \text{ mgL}^{-1}$ ) using ultra pure water (Millipore Milli-Q plus system, with a resistivity of  $18.2 \text{ M}\Omega \text{ cm}$  at  $25^\circ\text{C}$ ). Titanium dioxide with a constant loading of  $0.50 \text{ mg mL}^{-1}$  (Degussa P-25) was used as the photocatalyst. Mt (SAZ-1) and Kt (KGa-1b) were supplied from The Clay Minerals Society, Source Clays Repository (West Lafayette, IN). Mt (SAZ-1, cation exchange capacity (CEC):  $120 \text{ meq } 100 \text{ g}^{-1}$ , and  $\text{N}_2$ -BET surface area:  $97.42 \text{ m}^2 \text{ g}^{-1}$ ) and Kt (KGa-1b, CEC:  $2.0 \text{ meq } 100 \text{ g}^{-1}$ , and  $\text{N}_2$ -BET surface area:  $12.9 \text{ m}^2 \text{ g}^{-1}$ ) were used. Selected dose range of the clay minerals either as Mt or Kt was  $0.05$ – $0.2 \text{ mg mL}^{-1}$ .

### 2.2. Methodology

Bench-scale photocatalytic oxidation experiments were performed according to the methodology presented by Bekbolet and co-workers [12]. Following the photocatalytic treatment, all aqueous humic solutions were first centrifuged ( $5,000 \text{ rpm}$  for  $10 \text{ min}$ ) then the supernatants were filtered using a  $0.45 \mu\text{m}$  membrane filter (Millipore) to remove suspended particulate materials. Perkin–Elmer Lambda 35 UV–vis Spectrophotometer was used to record the UV–vis spectra and DOC ( $\text{mgL}^{-1}$ ) was measured using Total Organic Carbon Analyzer (Shimadzu TOC-VWP). As preliminary experiments, dark interactions (d) of HA and  $\text{TiO}_2$  in the presence of either Mt or Kt were assessed through experiments performed in the absence of irradiation. Photolytic removal of HA was also presented by the experiments performed in the absence of  $\text{TiO}_2$ . Moreover, binary interactions revealing the uptake of HA by  $\text{TiO}_2$ , Mt, or Kt were also assessed through baseline experiments that were carried out under dark conditions.

### 2.3. Specified and specific humic parameters

The parameters used for the elucidation of the photocatalytic oxidation of HA both in the presence and absence of clay minerals i.e. Mt or Kt were selected according to the UV–vis spectral properties. Absorbance measurements were performed at  $436 \text{ nm}$  ( $\text{Color}_{436}$ ),  $365 \text{ nm}$  ( $\text{UV}_{365}$ ),  $280 \text{ nm}$  ( $\text{UV}_{280}$ ), and  $254 \text{ nm}$  ( $\text{UV}_{254}$ ) [4]. Correspondingly specific parameters such as SCoA represents  $\text{Color}_{436}/\text{DOC}$ ,  $\text{SUVA}_{365}$  represents  $\text{UV}_{365}/\text{DOC}$ ,  $\text{SUVA}_{280}$  represents  $\text{UV}_{280}/\text{DOC}$ , and  $\text{SUVA}_{254}$  represents  $\text{UV}_{254}/\text{DOC}$ . Fractional UV–vis parameters were represented by the following ratios where for practical reasons, each E-term designates either UV or Color i.e.  $E_{254}/E_{365}$ ,  $E_{254}/E_{436}$ ,  $E_{280}/E_{365}$ ,  $E_{280}/E_{436}$ , and  $E_{365}/E_{436}$ . HA solution prepared at a concentration of  $50 \text{ mgL}^{-1}$  with a DOC content of  $17.00 \text{ mgL}^{-1}$  expressed  $\text{Color}_{436}$ :  $23.9 \text{ m}^{-1}$ ,  $\text{UV}_{365}$ :  $46.5 \text{ m}^{-1}$ ,  $\text{UV}_{280}$ :  $46.5 \text{ m}^{-1}$ , and  $\text{UV}_{254}$ :  $119.9 \text{ m}^{-1}$ .

## 3. Results and discussion

### 3.1. Evaluation of HA photocatalytic oxidation by UV–vis absorption spectra

Under the photocatalytic oxidation conditions, the UV–vis spectral properties of HA retained the basic declining features [4]. For comparison purposes, the UV–vis spectra were displayed for sole HA (A) and HA in the presence of Mt (B) and Kt (C) under photocatalytic oxidation conditions (Fig. 1(A–C)). In

general, UV–vis spectra of HA retained the logarithmic declining trend being different in absorbance magnitudes irrespective of the applied reaction conditions.

Bearing in mind that filtration through 0.45  $\mu\text{m}$  membrane filters consisted the major step of sample preparation following photocatalytic treatment and prior to the characterization analyses, the UV–vis spectra of HA (raw) and filtered HA (Rawf) were also given (Fig. 1(A–C)). Followed by photocatalysis (PC) (e.g. irradiation period of 60 min), oxidized HAs also retained the featureless declining trend. Since the figure covered only one single dose of clay mineral ( $0.1 \text{ mg mL}^{-1}$ ), it should be indicated that the UV–vis spectral shapes were under consideration rather than the extent of absorptivities that were obviously dose dependent.

The consistency attained in the UV–vis spectral shapes indicated the possibility of the implementation

of the specific as well as the fractional UV–vis parameters for the elucidation of the photocatalytic oxidation of HA under the specified experimental conditions.

### 3.2. Evaluation of HA photocatalytic oxidation by specific UV–vis absorbance parameters

As a basis to photocatalytic degradation, baseline and preliminary interactions were evaluated to express adsorptive interactions as well as photolytic removals. All of the specific UV–vis parameters displayed slight variations irrespective of the prevailing interaction mechanisms resulting from both preliminary and baseline interactions (Fig. 2 (A) and (B)). Dark interactions of HA and either Mt or Kt binary systems expressed lowest SCoA, and SUVA<sub>365</sub> whereas highest SUVA<sub>280</sub> and SUVA<sub>254</sub> were obtained upon dark

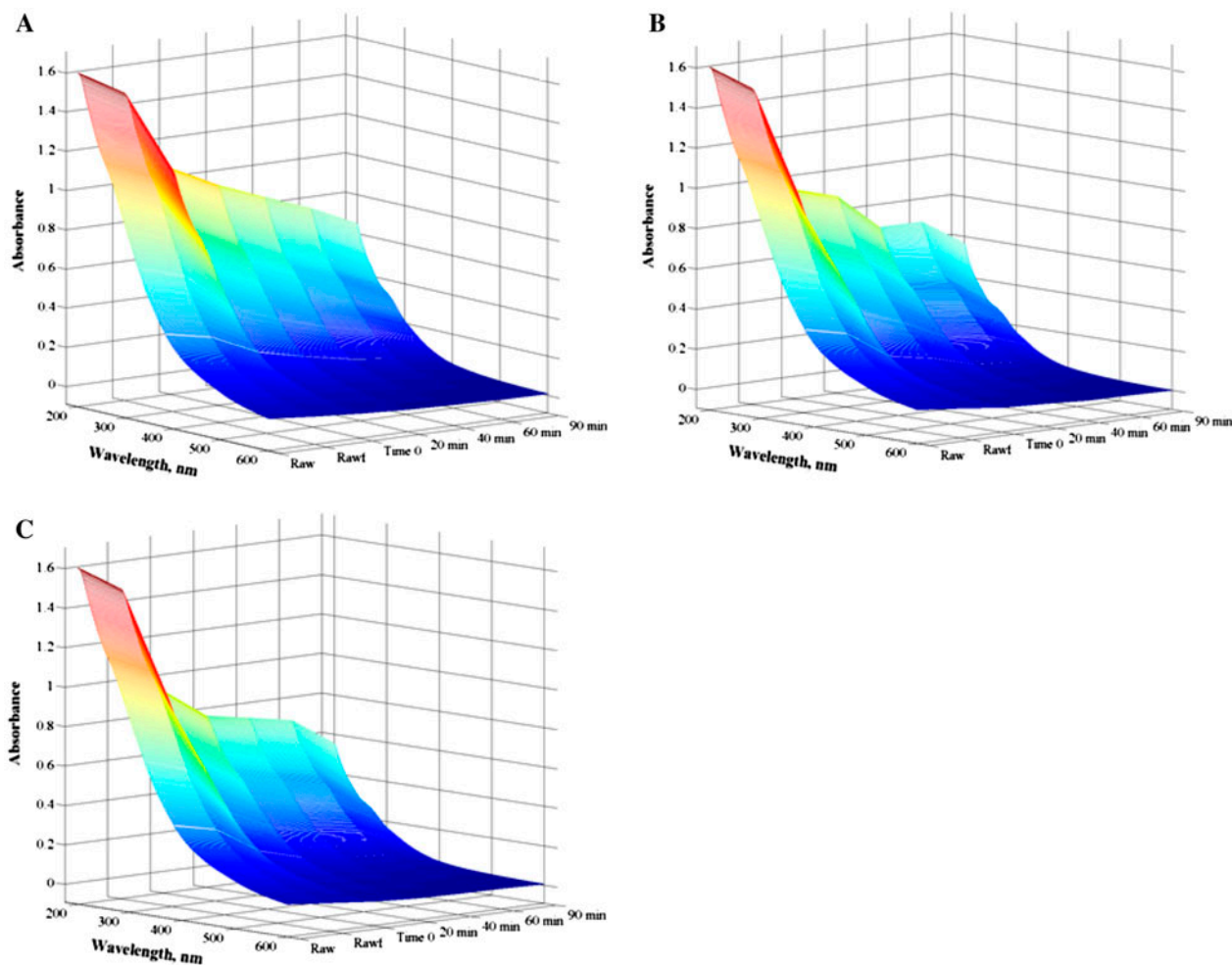


Fig. 1. UV–vis absorption profiles of (A) HA in the presence of Mt (B) (HA and Mt,  $0.1 \text{ mg mL}^{-1}$ ), Kt (C) (HA and Kt,  $0.1 \text{ mg mL}^{-1}$ ). Prior to and after photocatalysis (PC) (irradiation time: 0–60 min). For comparison purposes, samples were also presented followed by filtration through 0.45  $\mu\text{m}$  membrane filters (f).  $\text{TiO}_2$  loading was kept constant at  $0.50 \text{ mg mL}^{-1}$ .

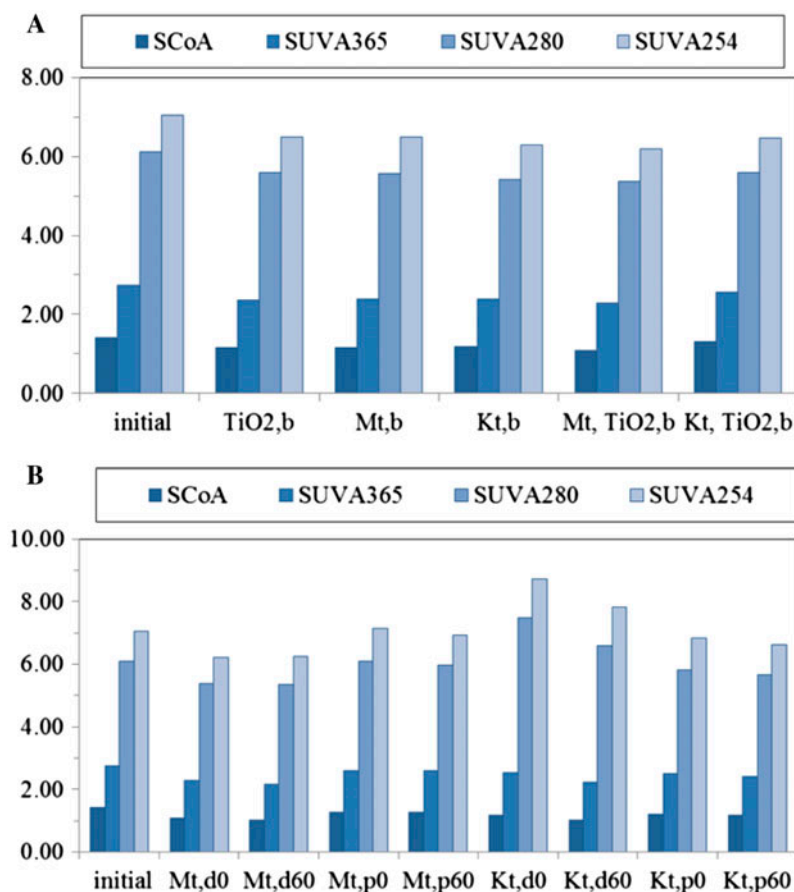


Fig. 2. Removal of specific UV-vis parameters of HA by baseline (A) and preliminary interactions (B) both in the presence and absence of clay minerals i.e. Mt/Kt. HA: 50 mg mL<sup>-1</sup>, Mt: 0.1 mg mL<sup>-1</sup>, Kt: 0.1 mg mL<sup>-1</sup>, TiO<sub>2</sub>: 0.5 mg mL<sup>-1</sup>, b: baseline interactions, d: dark interactions (time, 0 and 60 min), and p: photolytic interactions (irradiation time; 0 and 60 min).

interactions of HA and Kt binary system in the presence of TiO<sub>2</sub>. Considerably higher SUVA<sub>280</sub> and SUVA<sub>254</sub> indicated the dominating aromatic character of the residual HA fractions. The binary and ternary surface interactions resulted in successive removal of color-forming moieties rather than the counterpart's inner structural core aromatic domains with respect to the removals of DOC, under the specified experimental conditions. A plausible reason could be attributed to the prevailing electrostatic attractions between the charged humic functional groups and exposed surfaces of TiO<sub>2</sub>, Mt, and Kt.

Changes attained in the specific UV-vis parameters were also followed during photocatalytic degradation of HA both in the presence and absence of clay particles. It was observed that the removal of the specific UV-vis parameters revealed a logarithmic profile that could be successfully mimicked by a first-order kinetic decay model ( $R^2 > 0.80$ ) (Table 1). The possible role of the clay dose (0.05, 0.1, and 0.2 mg mL<sup>-1</sup>) due

to the presence of expanded surface exposed to the humic fractions was also presented. The expected effect could possibly be related to the enhanced

Table 1  
Photocatalytic first-order kinetic decay model rate constant ( $k \times 10^{-3} \text{ min}^{-1}$ ) of the specific UV-vis parameters of HA both in the presence and absence of either Mt or Kt

	Rate constant, $k \times 10^{-3}, \text{ min}^{-1}$			
	SUVA <sub>254</sub>	SUVA <sub>280</sub>	SUVA <sub>365</sub>	SCoA
HA	4.78	5.68	10.53	13.94
<i>Mt dose</i>				
0.05 mg mL <sup>-1</sup>	5.73	6.45	11.02	14.81
0.1 mg mL <sup>-1</sup>	6.33	7.26	13.35	18.66
0.2 mg mL <sup>-1</sup>	8.00	9.18	15.06	19.21
<i>Kt dose</i>				
0.05 mg mL <sup>-1</sup>	8.17	9.35	14.93	18.87
0.1 mg mL <sup>-1</sup>	6.24	7.23	11.70	15.07
0.2 mg mL <sup>-1</sup>	7.09	8.23	14.83	21.25

adsorptive interactions related to the increased surface area comprised of  $\text{TiO}_2$  as well as Mt and Kt.

Contrary to the effect observed in the presence of Kt, increasing Mt dose significantly affected the removal of the specific UV-vis parameters in a consistent trend. Regarding the different morphological properties of the clay minerals, it could be deduced that the mechanism of photocatalytic degradation proceeded through dissimilar pathways. On the other hand, photocatalytic degradation of sole HA displayed a consistent increasing trend for the removal of color-forming groups being faster with respect to the removal of the UV absorbing centers in accordance with the DOC removals.

### 3.3. Evaluation of HA degradation by fractional UV-vis parameters

Absorption of UV light by HA is caused by  $\pi$ -electrons and expresses conjugated aromatic systems,

whereas functional groups with quinoide structures and keto-enol-systems are more responsible for the visible light absorption [5]. Various absorption wavelengths at 254, 280, 365, 436, and 465 nm as well as ratios like E2/E3 (e.g.  $\text{UV}_{254}/\text{UV}_{365}$ ), E3/E4 (e.g.  $\text{UV}_{365}/\text{UV}_{436}$ ) have been reported as suitable parameters in the spectral differentiation of humic substances [4,5]. In a similar manner,  $E_{254}/E_{365}$ ,  $E_{254}/E_{436}$ ,  $E_{280}/E_{365}$ ,  $E_{280}/E_{436}$ , and  $E_{365}/E_{436}$  parameters have been selected for the differentiation of the prevailing systems under various conditions (Fig. 3).

Fig. 3(A) demonstrated the changes attained in the fractional UV-vis parameters of HA.  $E_{254}/E_{436}$  and  $E_{280}/E_{436}$  ratios displayed the most significant variations under baseline conditions. The reason could be attributed to the predominant role of the aromatic domains represented by  $\text{UV}_{254}$  and  $\text{UV}_{280}$  parameters with respect to the color-forming moieties ( $\text{Color}_{436}$ ).

Similar trends could also be visualized for the fractional UV-vis parameters of HA by preliminary

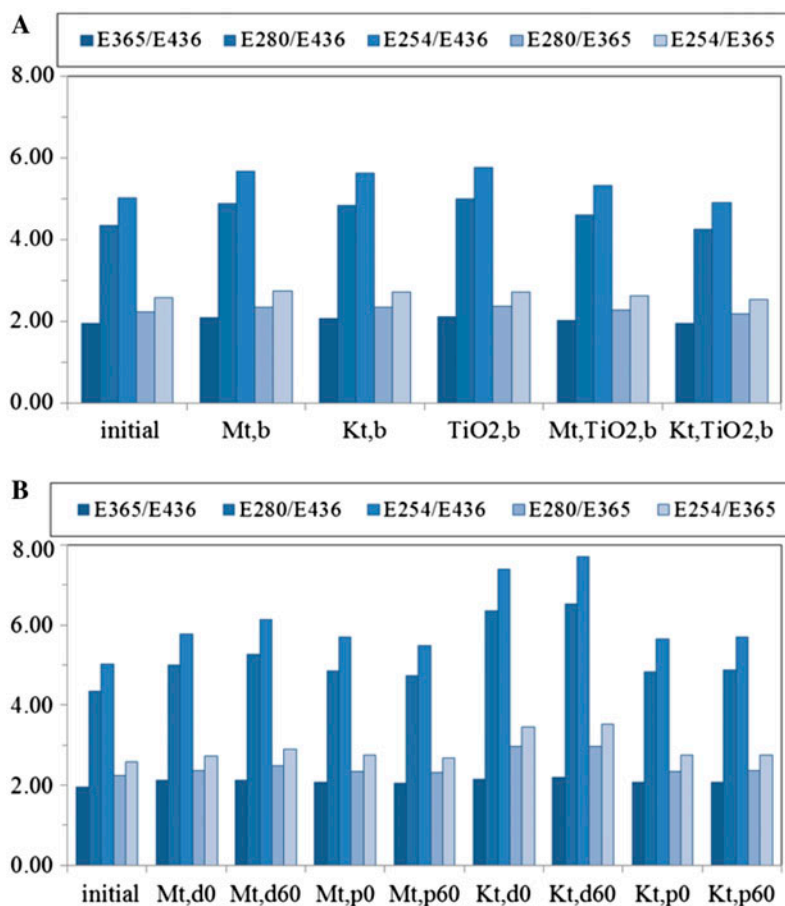


Fig. 3. Removal of fractional UV-vis parameters of HA by baseline (A) and preliminary (B) interactions both in the presence and absence of clay minerals i.e. Mt/Kt. HA:  $50 \text{ mg mL}^{-1}$ , Mt:  $0.1 \text{ mg mL}^{-1}$ ; Kt:  $0.1 \text{ mg mL}^{-1}$ ,  $\text{TiO}_2$ :  $0.5 \text{ mg mL}^{-1}$ , b: baseline interactions, d: dark interactions (time: 0 and 60 min) and p: photolytic interactions (irradiation time, 0 and 60 min).

experiments. Upon irradiation ( $t$ , 0–60 min) in the absence of  $\text{TiO}_2$ , comparatively similar changes in the fractional UV–vis parameters of HA were attained in the presence of either Mt or Kt expressing the sole photolytic behavior of HA irrespective of the aqueous medium constituents. However, due to the prevailing adsorption phenomena, time dependent changes in the humic fractional UV–vis parameters could be deduced being more significant in the presence of Kt with respect to the effect observed in the presence of Mt revealing the significant discriminative role of the surface properties of the clay minerals.

Furthermore, selected fractional UV–vis parameters were also followed, with respect to irradiation time during PC (Fig. 4(A–C)). The most significant differences were attained for  $E_{254}/E_{436}$ , and  $E_{280}/E_{436}$  revealing a differentiation between HA and HA-clay binary systems. The reason could be attributed to the prevailing competitive adsorption mechanism due to presence of  $\text{TiO}_2$  and either Mt or Kt. Depending on the irradiation conditions, both the unoxidized as well as the oxidized humic fractions could possibly be

attracted to the exposed oxide surfaces and further removed through filtration following photocatalytic treatment.

Although the presented figure (Fig. 4(A–C)) displays only one single dose of clay particles, in the presence of other doses of clay particles (0.05 and  $0.2 \text{ mg mL}^{-1}$ ), similar results were also attained.

### 3.4. Correlation between fractional UV–vis and specific UV–vis parameters

UV–vis absorptions measured at 365 and 446 nm (E3 and E4, respectively) and their ratio (E3/E4) were presented with respect to the changes attained in the respective specific UV–vis parameters as SCoA and  $\text{SUVA}_{365}$ . These two-variables displayed the following tendency as the higher the specific absorption, the lower was the E3/E4 absorption ratio for HAs [13]. The observed phenomenon was attributed to a possible indication of an increasing aromaticity and molecular weight of HAs. The overall evaluation would indicate the persistence of basic humic properties

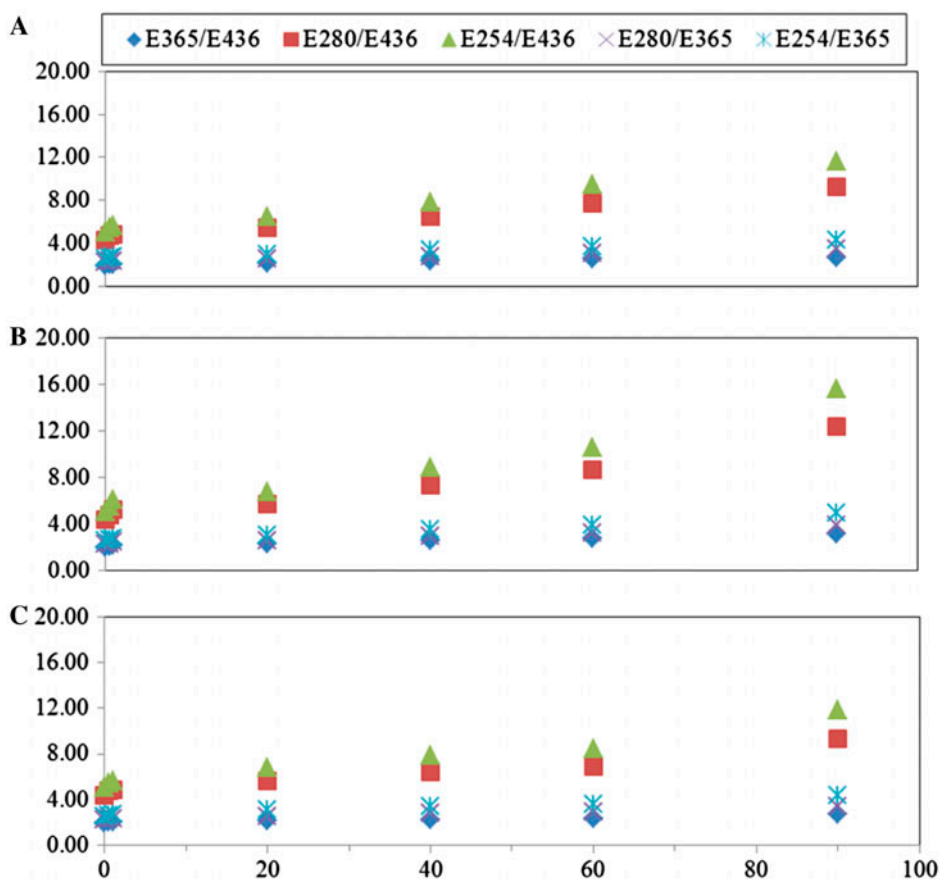


Fig. 4. (A)–(C). Change of fractional UV–vis parameters of HA with respect to irradiation time (x-axis, irradiation time: 0–90 min) both in the presence and absence of clay minerals i.e. Mt/Kt. (A): HA, (B): HA and Mt, and (C): HA and Kt. (HA:  $50 \text{ mg mL}^{-1}$ , Mt:  $0.1 \text{ mg mL}^{-1}$ , Kt:  $0.1 \text{ mg mL}^{-1}$ ,  $\text{TiO}_2$ :  $0.5 \text{ mg mL}^{-1}$ ).

rather than the formation of lower molecular weight oxidized and more fulvic-like structure, with reference to the expected range of  $E_{365}/E_{436} > 4$ . The relationships were displayed where  $E_{365}/E_{436}$  and  $E_{254}/E_{436}$  were correlated with the respective specific UV–vis parameters as SCoA, SUVA<sub>365</sub>, and SUVA<sub>254</sub> (Fig. 5 (A) and (B)).

$E_{365}/E_{436}$  ratio displayed a discriminative behavior with respect to SUVA<sub>365</sub> and SCoA values of the clay minerals either for Mt or Kt. However, the variations observed in SCoA and SUVA<sub>254</sub> with respect to  $E_{254}/E_{436}$  did not reveal any significant difference from clay type point of view. Moreover, the attained data could well be modeled by a linear relationship irrespective of the clay type;

$$\text{SUVA}_{254} = -0.12(E_{254}/E_{436}) + 1.81 (r^2 = 0.84)$$

$$\text{SCoA} = -0.11(E_{254}/E_{436}) + 1.72 (r^2 = 0.80)$$

In the presence of Mt, SCoA, and SUVA<sub>365</sub> relationships with respect to  $E_{365}/E_{436}$  could be expressed by the following Eqs. (1) and (2)

$$\text{SCoA} = -0.65(E_{365}/E_{436}) + 2.58 \quad r^2 = 0.89 \quad (1)$$

$$\text{SUVA}_{365} = -1.16(E_{365}/E_{436}) + 4.95 \quad r^2 = 0.91 \quad (2)$$

In the presence of Kt, SCoA, and SUVA<sub>365</sub> relationships with respect to  $E_{365}/E_{436}$  could be expressed by the following Eqs. (3) and (4)

$$\text{SCoA} = -0.85(E_{365}/E_{436}) + 2.78 \quad r^2 = 0.80 \quad (3)$$

$$\text{SUVA}_{365} = -1.51(E_{365}/E_{436}) + 5.28 \quad r^2 = 0.80 \quad (4)$$

Moreover, in the presence of Mt, SCoA, and SUVA<sub>254</sub> relationships with respect to  $E_{254}/E_{436}$  could be expressed by the following Eqs. (5) and (6)

$$\text{SCoA} = -0.11(E_{254}/E_{436}) + 1.64 \quad r^2 = 0.895 \quad (5)$$

$$\text{SUVA}_{254} = -0.32(E_{254}/E_{436}) + 8.07 \quad r^2 = 0.91 \quad (6)$$

Also, in the presence of Kt, SCoA, and SUVA<sub>254</sub> relationships with respect to  $E_{254}/E_{436}$  could be expressed by the following Eqs. (7) and (8)

$$\text{SCoA} = 0.09(E_{254}/E_{436}) + 1.54 \quad r^2 = 0.79 \quad (7)$$

$$\text{SUVA}_{254} = -0.29(E_{254}/E_{436}) + 7.84 \quad r^2 = 0.82 \quad (8)$$

Regarding the close similarities of the coefficients of Eqs. (5) and (7) and Eqs. (6) and (8), the attained overall data could well be modeled by a linear relationship irrespective of the clay type as given in below Eqs. (9) and (10):

$$\text{SCoA} = 0.11(E_{254}/E_{436}) + 1.72 \quad r^2 = 0.80 \quad (9)$$

$$\text{SUVA}_{254} = -0.32(E_{254}/E_{436}) + 8.29 \quad r^2 = 0.84 \quad (10)$$

It is noteworthy to indicate that the correlation of SCoA and SUVA<sub>254</sub> parameters with respect to  $E_{254}/E_{436}$  did not reveal any significant differences from the clay-type point of view. Therefore, both

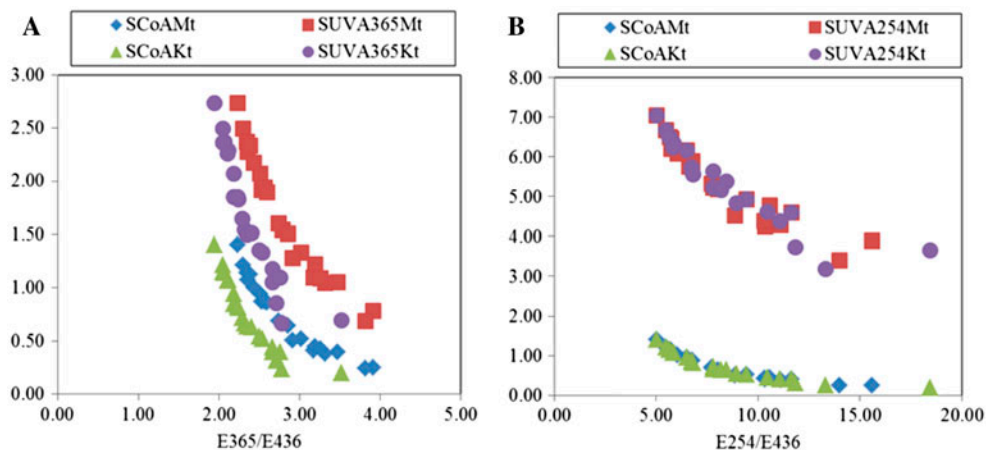


Fig. 5. (A) Specific SCoA and SUVA<sub>365</sub> variation with respect to  $E_{365}/E_{436}$  ratio of HA and (B) Specific SCoA and SUVA<sub>254</sub> variation with respect to  $E_{254}/E_{436}$  ratio of HA in the presence of Mt or Kt upon PC irrespective of clay dose and irradiation conditions.

SCoA and SUVA<sub>365</sub> parameters could well be correlated with E<sub>365</sub>/E<sub>436</sub> to express the discrimination of the effects of the different clay minerals. It should also be mentioned that neither irradiation period nor dose of the clay minerals contributes remarkably on the correlation. As a conclusive remark, color-forming moieties (Color<sub>436</sub>) as well as the UV absorbing centers at near visible wavelength (UV<sub>365</sub>) as related to the DOC removals could serve as a differentiation factor for the assessment of the effects of the clay minerals on the photocatalytic degradation of HAs.

#### 4. Conclusion

UV-vis spectral features of sole HA and HA in the presence of either Mt or Kt were elucidated both under non-oxidative and photocatalytic oxidation conditions. The study demonstrated the use of specific UV-vis (i.e. SCoA, SUVA<sub>365</sub>, SUVA<sub>280</sub>, and SUVA<sub>254</sub>) and fractional UV-vis parameters (i.e. E<sub>254</sub>/E<sub>365</sub>, E<sub>254</sub>/E<sub>436</sub>, E<sub>280</sub>/E<sub>365</sub>, E<sub>280</sub>/E<sub>436</sub>, and E<sub>365</sub>/E<sub>436</sub>) of HA for the visualization of the photocatalytic oxidation process. The variations attained in SCoA and SUVA<sub>254</sub> with respect to E<sub>254</sub>/E<sub>436</sub> did not reveal any significant discrimination from clay-type point of view, hence could well be modeled by a linear relationship irrespective of the clay type. On the other hand, the relationship of E<sub>365</sub>/E<sub>436</sub> and SUVA<sub>365</sub> and SCoA parameters displayed a discriminative behavior with respect to the type of the clay mineral as represented by the correlation equations. As a conclusive remark, it could be indicated that under nonselective oxidation conditions, besides the determination of the DOC contents of the oxidized HA fractions and UV-vis spectroscopic investigation as a non-destructive simple technique could still hold importance for the elucidation of the effects of the complex reaction medium as demonstrated for clay minerals.

#### References

- [1] J.A. Leenheer, J-P Croué, Characterizing aquatic dissolved organic matter, *Environ. Sci. Technol.* 37 (2003) 18A–26A.
- [2] E. Boyle, N. Guerriero, A. Thiallet, R. Del Vecchio, N.V. Blough, Optical Properties of humic substances and CDOM: Relation to structure, *Environ. Sci. Technol.* 43 (2009) 2262–2268.
- [3] M. Fuentes, G. González-Gaitano, J.M. García-Mina, The usefulness of UV-visible and fluorescence spectroscopies to study the chemical nature of humic substances from soils and compounds, *Org. Geochem.* 37 (2006) 1949–1959.
- [4] C.S. Uyguner, M. Bekbolet, Evaluation of humic acid photocatalytic degradation by UV-vis and fluorescence spectroscopy, *Catal. Today* 101 (2005a) 267–274.
- [5] C.S. Uyguner, M. Bekbolet, Implementation of spectroscopic parameters for practical monitoring of natural organic matter, *Desalination* 176 (2005b) 47–55.
- [6] C.S. Uyguner, M. Bekbolet, A review on the photocatalytic degradation of humic substances, in: A. Nikolau, H. Selcuk, L. Rizzo, in: *Control of Disinfection By-products in Drinking Water Systems*, NOVA Science Publishers Inc., New York, NY, 2007, pp. 419–446.
- [7] C.S. Uyguner-Demirel, M. Bekbolet, Significance of analytical parameters for the understanding of natural organic matter in relation to photocatalytic oxidation, *Chemosphere* 84 (2011) 1009–1031.
- [8] S. Sen Kavurmaci, M. Bekbolet, Photocatalytic degradation of humic acid in the presence of montmorillonite, *Appl. Clay Sci.* 75–76 (2013) 60–66.
- [9] S. Sen Kavurmaci, M. Bekbolet, Non-selective oxidation of humic acid in heterogeneous aqueous systems: A comparative investigation between montmorillonite and kaolinite, (2013) (Submitted for publication).
- [10] C.W. Li, M.M. Benjamin, G.V. Korshin, Use of UV spectroscopy to characterize reactions between NOM and free chlorine, *Environ. Sci. Technol.* 34 (2000) 2570–2575.
- [11] J.L. Weishaar, G.R. Aiken, B.A. Bergamaschi, M.S. Fram, R. Fujii, K. Mopper, Evaluation of specific ultraviolet absorbance as an indicator of the chemical composition and reactivity of dissolved organic carbon, *Environ. Sci. Technol.* 37 (2003) 4702–4708.
- [12] M. Bekbolet, A.S. Suphandag, C.S. Uyguner, An investigation of the photocatalytic efficiencies of TiO<sub>2</sub> powders on the decolourisation of humic acids, *J. Photochem. Photobiol., A* 148 (2002) 121–128.
- [13] R. Artinger, G. Buckau, S. Geyer, P. Fritz, M. Wolf, J.I. Kim, Characterization of groundwater humic substances: Influence of sedimentary organic carbon, *Appl. Geochem.* 15 (2000) 97–116.